Clim Dyn
DOI 10.1007/s00382-015-2563-8

PDO modulation of ENSO effect on tropical cyclone rapid intensification in the western North Pacific

Xidong Wang[1] · **Hailong Liu**[2,3]

Received: 15 October 2014 / Accepted: 14 March 2015

Abstract This study investigates how the Pacific Decadal Oscillation (PDO) modulates the effect of El Niño/Southern Oscillation (ENSO) on tropical cyclone rapid intensification (RI) in the western North Pacific. The analysis shows that the interannual relationship between ENSO and annual RI number in warm PDO phases is strong and statistically significant. In cold PDO phases, however, there is no significant correlation between ENSO and RI on the interannual timescale. The enhancement of the interannual ENSO–RI relationship in warm PDO phases is mainly attributable to the change of the environmental vertical wind shear. The PDO in warm (cold) phases can strengthen (weaken) an El Niño event to increase (reduce) the effects of the warm pool of water over the equatorial Pacific in typhoon season by local diabatic heating. El Niño events are accompanied by the stronger Walker circulation in the equatorial Pacific in the warm PDO phase than in the cold PDO phase. In contrast, the Walker circulation pattern and amplitude associated with La Niña events is less affected by the alternate PDO phase. This tends to make the atmospheric response to ENSO stronger (weaker) in warm (cold) PDO phase, and so is the atmospheric teleconnection of ENSO. Our results indicate that the stratification of ENSO-based statistical RI forecast by the PDO can greatly improve the accuracy of statistical RI predictions.

Keywords El Niño/Southern Oscillation · Pacific Decadal Oscillation · Tropical cyclone · Rapid intensification

1 Introduction

The tropical cyclone (TC) rapid intensification (RI) is a universal feature of the category 4 and 5 TCs on the Saffir-Simpon scale, which is one of the greatest challenges in TC prediction. It is usually defined as an increase in maximum sustained wind speeds of at least 15.4 m/s (30 kt) in a 24-h period (Kaplan and DeMaria 2003). Over the western North Pacific (WNP), the category 4 and 5 TCs are called super typhoons (STs), 90 % of which undergo at least one RI process (Wang and Zhou 2008, hereafter referred to WZ08). Over the North Atlantic basin, all category 4 and 5 hurricanes in their lifetimes experience at least one RI event (Kaplan and DeMaria 2003). It is argued that a great amount of property damage and casualties produced by TCs can be attributed to RI (Lin et al. 2008). As is stressed by WZ08, the importance of studying the climate modulation of RI cannot be overemphasized.

The influences of different El Niño/Southern Oscillation (ENSO) phases on TC activities in the WNP, have been extensively investigated (Wang and Chan 2002; Camargo and Sobel 2005; Kim et al. 2011; Li and Zhou 2012; Wang et al. 2013; Wang and Wang 2013). The genesis frequency during the El Niño phase increases over the southeastern part of the WNP and decreases over the northwestern part. La Niña phase causes an opposite situation (Wang and Chan 2002). Li and Zhou (2012) separated TCs into three

✉ Xidong Wang
xidong_wang@yahoo.com

[1] Key Laboratory of Marine Environmental Information Technology, SOA, National Marine Data and Information Service, 93 Liuwei Road, Hedong District, Tianjin 300171, China

[2] Cooperative Institute for Marine and Atmospheric Studies, University of Miami, Miami, FL, USA

[3] NOAA/Atlantic Oceanographic and Meteorological Laboratory, Miami, FL, USA

Published online: 24 March 2015

groups including super typhoons, typhoons, and tropical storms and tropical depressions to investigate the relationship with ENSO. They found that an increase (decrease) in the frequency of super typhoons is usually associated with the mature phase of El Niño (La Niña) events, while the converse is true for tropical storms and tropical depressions. Due to the effect of ENSO on annual mean lifetime, intensity, and number of TCs, accumulated cyclone energy (ACE) is positively correlated with ENSO (Camargo and Sobel 2005). In addition to TC number, lifetime and intensity, track and landfall of TCs is also related to the phase of ENSO. During El Niño, TCs tend to form in the farther east of the WNP, which induces TCs to more recurve toward higher latitudes. However, during La Niña, TCs tends to extend more westward, increasing probability of landfall over China (Elsner and Liu 2003; Camargo et al 2007; Kim et al 2011). Due to the different spatial location of the warm sea surface temperature (SST) anomaly, several studies have found that El Niño can be classified into two types: the canonical El Niño (or East Pacific Warimg) and El Niño Modoki (or Central Pacific Warming). Maximum warm SST anomaly of the former is confined to the east Pacific whereas the latter has maximum warm SST anomaly near the dateline. El Niño Modoki with the shifting of the warm SST anomaly shows to induce remote climate anomalies over the globe that are significantly different from those produced by the canonical El Niño (Ashok et al. 2007; Ashok and Yamagata 2009; Weng et al. 2007, 2009; Kao and Yu 2009; Kug et al. 2009; Yeh et al. 2009). Moreover, Kim et al. (2011) have found that the two types of El Niño differently affect the genesis and tracks of TCs over the WNP. In the canonical El Niño years, the genesis and the track density of TCs tend to be enhanced over the southeastern part of the WNP and suppressed in the northwestern part of the WNP. In the El Niño Modoki years, the TC activity is shifted to the west and is extended through the northwestern part of the WNP. Furthermore, Wang et al. (2013) examined different impacts of canonical El Niño and El Niño Modoki events on the genesis, intensity, and tracks of TCs in the WNP by considering the early season of April–June, the peak season of July–September and the late season of October–December. Based on the opposite influences on rainfall in southern China during boreal fall, Wang and Wang (2013) classified El Niño Modoki into two groups: El Niño Modoki I and II, which shows different origins and patterns of SST anomalies. Differing from canonical El Niño and El Niño Modoki I, El Niño Modoki II corresponding to northwesterly anomalies of the typhoon steering flow is unfavorable for typhoons to make landfall in China. Recently, different effects of the canonical El Niño and El Niño Modoki on TC genesis over the South China Sea (SCS) was also investigated (Wang et al. 2014). TC genesis is significantly related with the El Niño Modoki index, but not with the canonical El Niño index. It is found that in the past two decades the SCS TC genesis varies consistently with the El Niño Modoki index on a timescale of about 4 years, which is coherent with the recent increase in El Niño Modoki events (Wang et al. 2014).

These studies above mainly focused on the influence of ENSO on the genesis, tracks, duration and intensity of TCs. Few studies have attempted to investigate the climate modulation on RI variability. Recently using the TC best-track data during 1965–2004, WZ08 identified the importance of climatic conditions to the frequency and location of RI occurrences and found that the mean number of RI in El Niño years is significantly higher than that in La Niña years. Previous studies suggested that the interannual relationship between ENSO and the global climate appears as a nonstationary state (Wang et al. 2008), which can be ascribed to the Pacific Decadal Oscillation (PDO). The PDO can modulate the frequency and strength of ENSO phases, and then cause different thermodynamic and dynamic conditions of the ocean and atmosphere (Kurtzman and Scanlon 2007). For example, the relationship between ENSO and the East Asian summer monsoon during 1962–1977 was found to be significantly different from that during 1978–1993 (Wu and Wang 2002), which actually corresponds to an evolution of the PDO (Wang et al. 2008). Yu and Zwiers (2007) found that both the tropospheric circulation and the North American temperature suggested an enhanced Pacific North America-like climate response when ENSO and the PDO vary in phase. Wang et al. (2008) investigated the modulated effect of ENSO by the PDO on the East Asian winter monsoon and discovered that there is no robust relationship between ENSO and the East Asian winter monsoon on the interannual timescale when the PDO is in its warm phase. However, when the PDO is in its cold phase, ENSO can exert a strong effect on the East Asian winter monsoon, with robust and significant low-level temperature changes occurring over East Asia. Krishnamurthy and Krishnamurthy (2013) found that the PDO can extend its influence to the tropical Pacific to modify the relationship between the Southern Asian summer monsoon and ENSO.

Due to multi-decadal modulation of the PDO on atmospheric and oceanic states, one question arises whether the interannual effect of ENSO on TC RI changes with the evolution of the PDO phase. This study therefore makes an effort to examine the PDO modulation of the interannual ENSO–RI relationship, which has not been systematically studied in the literature.

The rest of this paper is organized as follows. The datasets used in this paper are introduced in Sect. 2. Section 3 investigates how the PDO affects the interannual ENSO–RI relationship. Section 4 discusses mechanism by which the PDO modulates the effects of ENSO on large-scale environments related to RI. Summary and discussion are given in Sect. 5.

2 Data

The 6-h TC best-track over the WNP is obtained from the Joint Typhoon Warning Center to identify the occurrence of the RI. The intensity change threshold of 30 kt/24 h is employed to define the RI events (e.g., Kaplan and DeMaria 2003; Kaplan et al. 2010; Shu et al. 2012). The monthly dataset of the Extended Reconstruction SST (ERSST) is obtained from the National Climatic Data Center (NODC), National Oceanic and Atmospheric Administration (NOAA). The horizontal resolution is 2° × 2° (Smith et al. 2008). The tropical cyclone heat potential (TCHP), vertical wind shear (VWS) between 850 and 200 hPa and relative humidity (RHUM) in the 500 hPa are investigated in order to examine the large-scale environments associated with RI. TCHP is defined as the ocean heat content contained in waters warmer than 26 °C. It is calculated by using the temperature–salinity from the Simple Ocean Data Assimilation (SODA) which is based on the Parallel Ocean Program ocean model with an average horizontal resolution of 0.5 × 0.5 and with 40 vertical levels.

The atmospheric variables including winds in the 850 and 200 hPa, RHUM in the 500 hPa are from twentieth century reanalysis version 2 (20CRv2), which contains the synoptic-observation based estimate of global tropospheric variability at monthly temporal and 2° × 2° spatial resolutions (Compo et al. 2011). VWS is calculated as the magnitude of the vector difference between monthly mean winds at 850 and 200 hPa. The vertical profile of the divergent component of zonal winds averaged between 5°S and 5°N represents walker circulation. The averaged TCHP, VWS, and RHUM for May–November are linearly detrended prior to analysis.

The overlapping bimonthly mean multivariate ENSO index (MEI) is obtained from the Climate Diagnostic Center of NOAA (Wolter and Timlin 1998). The PDO index is constructed by using the ERSST from the National Ocean Data Center, which is defined as the leading principal component of monthly SST anomalies in the North Pacific Ocean poleward of 20°N (Mantua et al. 1997). The MEI and PDO indexes for the months of May–November are averaged to represent the status of ENSO and the PDO during active TC seasons.

3 Results

3.1 ENSO effect on RI

To identify the relationship between RI and ENSO, Fig. 1a displays the standardized annual RI number and May–November-averaged MEI index during 1951–2008. The simultaneous correlation between the annual RI number and MEI index is calculated. The annual RI number

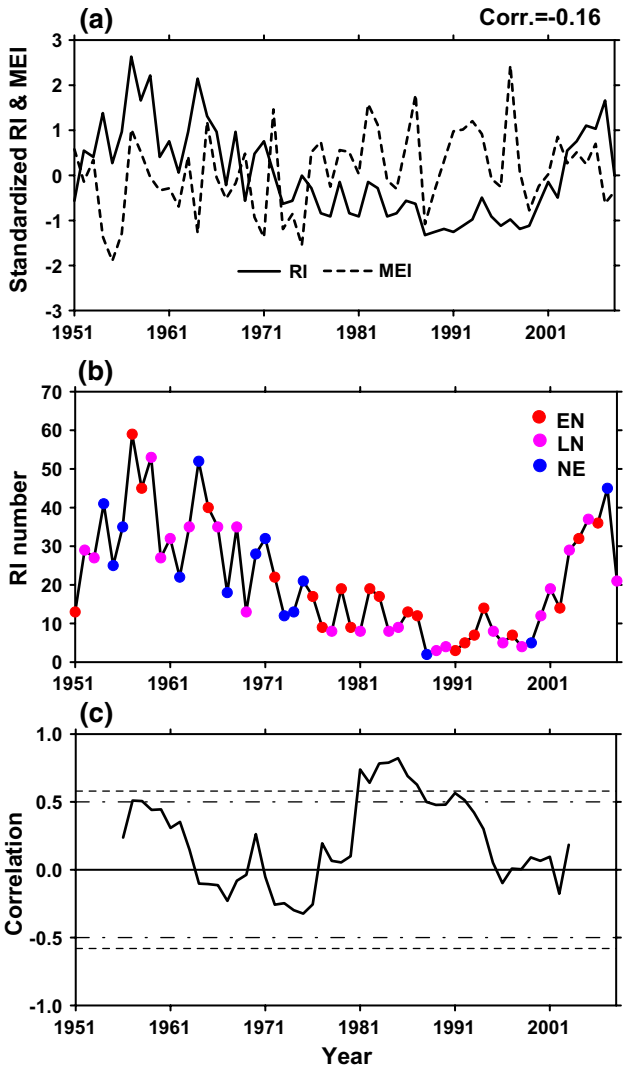

Fig. 1 **a** Time series of averaged-May–November MEI index and standardized annual RI number. **b** Time series of annual RI number. EN, LN, and NE represents the El Niño years, La Niña and neutral years, respectively. **c** 10-year sliding correlation between averaged-May–November MEI index and annual RI number during 1951–2008. The *dash line* and *dash dot line* indicate 90 and 95 % confidence level, respectively

is negatively correlated with MEI, but is not statistically significant at the 95 % confidence level. Based on such a simple correlation analysis, it is vague to determine the ENSO effect on the annual number of RI. To clarify the ENSO effect, we group the years of the entire period into El Niño (MEI ≥ 0.5), La Niña (MEI ≤ −0.5) and neutral years (−0.5 < MEI < 0.5), and then we get 21, 23, and 14 years classified as El Niño, La Niña and neutral years, respectively. The annual RI number in the different ENSO phases is shown in Fig. 1b. Over the WNP, the average RI number in the El Niño years is 19.6, which is lower than that (25.1) in the La Niña years. Averaged RI number in the

Table 1 Classification of years by ENSO phase and PDO phase based on the averaged-May–November MEI and PDO indices during 1951–2008

ENSO phase	Warm PDO phase (1979–1997)	Cold PDO phase (1951–1978 and 1998–2008)
El Niño year	1979(19), 1980(9), 1982(19), 1983(17), 1986(13), 1987(12), 1991(3), 1992(5), 1993(7), 1994(14), 1997(7)	1951(13), 1957(59), 1958(45), 1965(40), 1972(22), 1976(17), 1977(9), 2002(14), 2006(36)
	Average RI number: 11.3	Average RI number: 28.3
La Niña year	1988(2)	1954(41), 1955(25), 1956(35), 1962(22), 1964(52), 1967(18), 1968(35),1970(28),1971(32),1973(12),1974(13), 1975(21), 1999(5), 2007(45)
	Average RI number: 2	Average RI number: 27.4

The RI number is provided in parentheses

neutral years is 20.0. The standard deviations of 14.7, 14.8 and 14.0 in three ENSO phases are comparable.

In order to examine the sensitivity of the relationship between ENSO and RI to the ENSO phase definition, we select eight strong El Niño years (1957, 1965, 1972, 1982, 1983, 1987, 1992, 1997) and eight strong La Niña years (1954, 1955, 1956, 1964, 1971, 1973, 1975, 1988) according to the criteria that the absolute value of MEI exceeds a unit during 1951–2008. The annual mean number of RI in the eight La Niña years is 27.5, which surpasses that (22.6) in the eight El Niño years. Mean difference of RI numbers between La Niña and El Niño years based on both of the two different ENSO definition criteria are statistically significant at the 95 % confidence level using a Student's *t* test. Therefore, it suggests that our results are not sensitive to the ENSO phase criteria that we choose.

However, the above conclusion will not hold true if we chose the study period of 1965–2004. The seven El Niño (1965, 1972, 1982, 1987, 1991, 1997, and 2002) and La Niña (1970, 1971, 1973, 1975, 1988, 1998 and 1999) years during 1965–2004 are chosen as in WZ08 to investigate the ENSO effect on RI. Then the annual mean number of RI in the El Niño years is higher than that in the La Niña years, which is in agreement with WZ08 but leads to the opposite conclusion to the study based on the period of 1951–2008. This discrepancy may be mainly attributed to the difference in the length of TC time series examined. Thus, it also indicates that the ENSO effect on RI is time dependent.

3.2 PDO modulation of ENSO effect on RI

A 7-year Gaussian filter is performed to obtain multi-decadal variability of the PDO. We obtain two cold phase periods with low PDO values: 1951–1978 (period I), 1998–2008 (period III), and a warm phase period with high PDO values: 1979–1997 (period II), which are consistent with previous studies (e.g., Wang et al. 2009). The partition of RI variation according to the phases of ENSO and the PDO are exhibited in Table 1. The occurrence frequency of La Niña events in two cold PDO phases during periods I and III is much higher than that in the warm PDO phase during period II. During the total 39 years of the two cold phases, La Niña events amount to 14, accounting for about 36 % of 39 years. However, during the total 19 years of the warm PDO phase, only one La Niña event takes place, just accounting for 5 % of 19 years. For the other phase of ENSO, the occurrence frequency of El Niño events in two cold PDO phases is lower that in the warm PDO phase. The nine El Niño events in two cold PDO phases account for about 24 % of 39 years whereas 11 out of the 19 years in the warm PDO phase are El Niño years, making up about 58 % of the total 19 years. Therefore, it is pronounced that the change of ENSO activity can partly originate from the alternation of the PDO phases, which agrees with previous studies (e.g., Verdon and Franks 2006; Kurtzman and Scanlon 2007; Wang et al. 2009).

Furthermore, an evident modulation of the PDO on the interannual ENSO–RI relationship can be identified. When El Niño and La Niña events are occurring in the same PDO phase, the annual mean number of RI in El Niño years is higher than that in La Niña years. However, a total of 11 years classified as El Niño events when the PDO is in its warm phase, have low-average annual RI number. In contrast, five of the 9 years that have El Niño conditions, when the PDO is its cold phase, have annual RI number exceeding the average during 1951–2008 (21.1). For example, 1957, 1958, and 1965 TC seasons are characterized by annual RI number of greater than twice of the 1951–2008 average (21.1). Only one out of 19 years in the warm PDO phase classified as La Niña has annual RI number lower than the average during 1951–2008, while nine of the 14 years that have La Niña conditions when the PDO is in its cold phase have annual RI number above the average. All differences discussed above are statistically significant at the 95 % confidence level excluding the difference between El Niño-cold PDO and La Niña-warm PDO. Figure 1c shows a 10-year sliding correlation between May–November-averaged MEI index and annual RI number. It is clearly shown in Fig. 1c that the interannual ENSO–RI relationship seems to be random over most periods from 1951 through to 2008 (except for the 1980s–1990s) without any discernibly significant

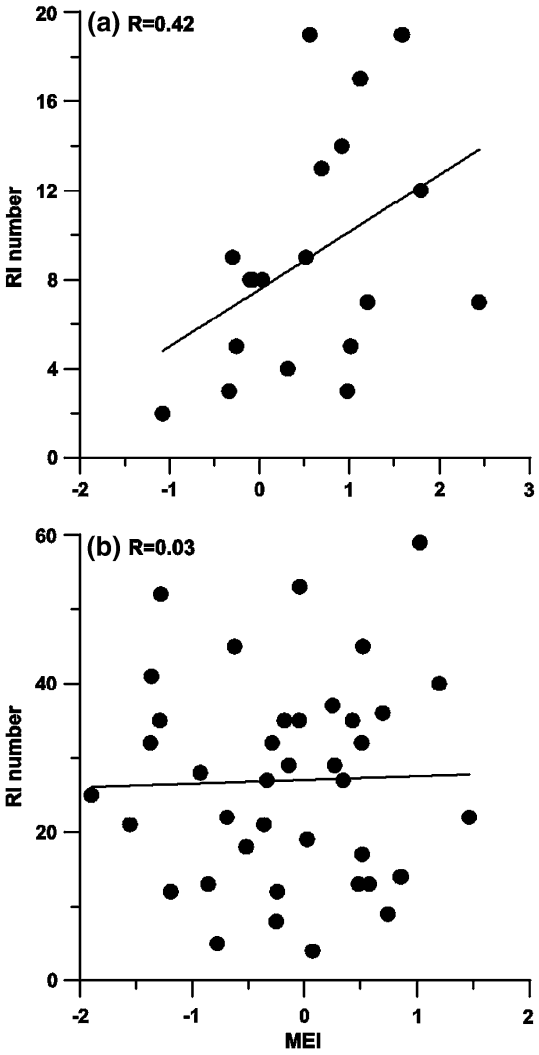

Fig. 2 Scatter diagrams between the averaged-May–November MEI and annual RI number for the **a** warm and **b** cold PDO phase. The *thick line* is the linear regression

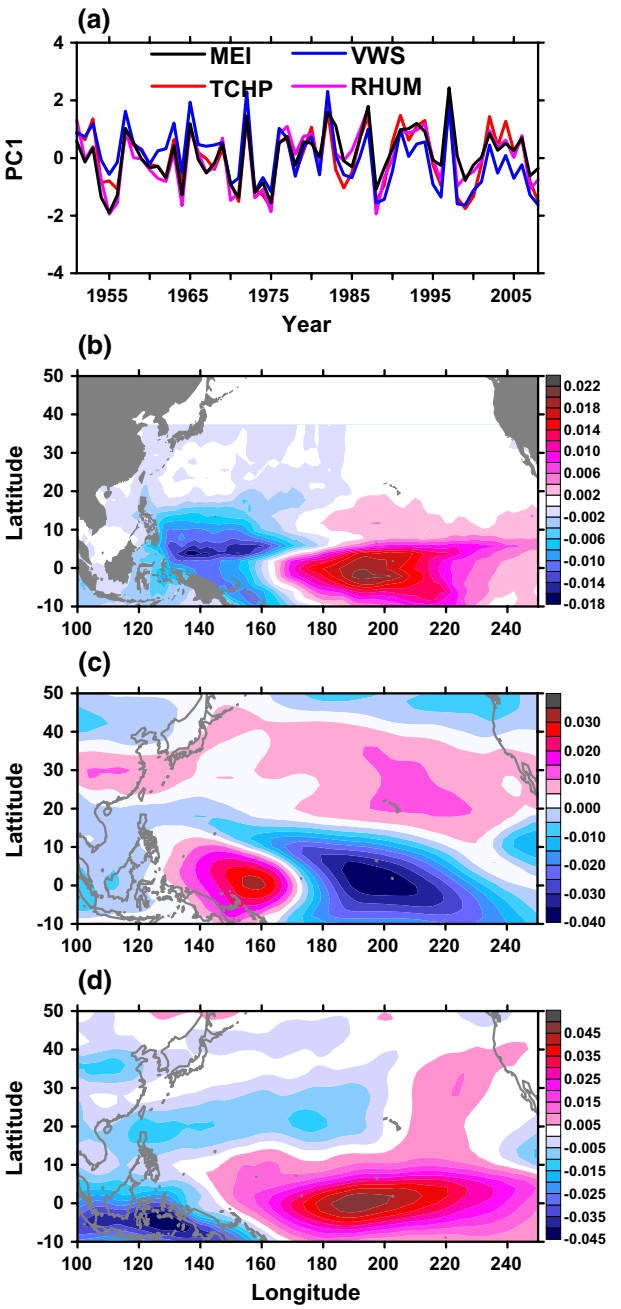

Fig. 3 PC1 and EOF1 of the averaged-May–November TCHP, VWS, and RHUM during 1951–2008

correlation. However, in 1980s–1990s when the PDO is in its warm phase, the interannual ENSO–RI correlation becomes statistically significant. Figure 2 further shows the scatter plots between MEI index and annual RI number in different PDO phases. It is found that the MEI in the warm PDO phase is significantly correlated with annual RI number at the 90 % confidence level whereas there is no significant correlation in cold PDO phase. Therefore it suggests that during the warm PDO phase, ENSO can exert much stronger influence on the interannual variability of RI.

4 Physical interpretations

Why the interannual relationship between ENSO and RI has changed with the different PDO phases need to be addressed. We start from exploring the corresponding oceanic and atmospheric conditions associated with RI by using Empirical Orthogonal Function (EOF) analysis on May–November averaged TCHP, VWS and RHUM. Figure 3 shows the standardized first principal component (PC1) time series and EOF1 of the TCHP, VWS and RHUM. Their PC1s are highly correlated with the MEI index, with correlation coefficients of 0.84, 0.90, and 0.88, respectively. All correlations are statistically significant

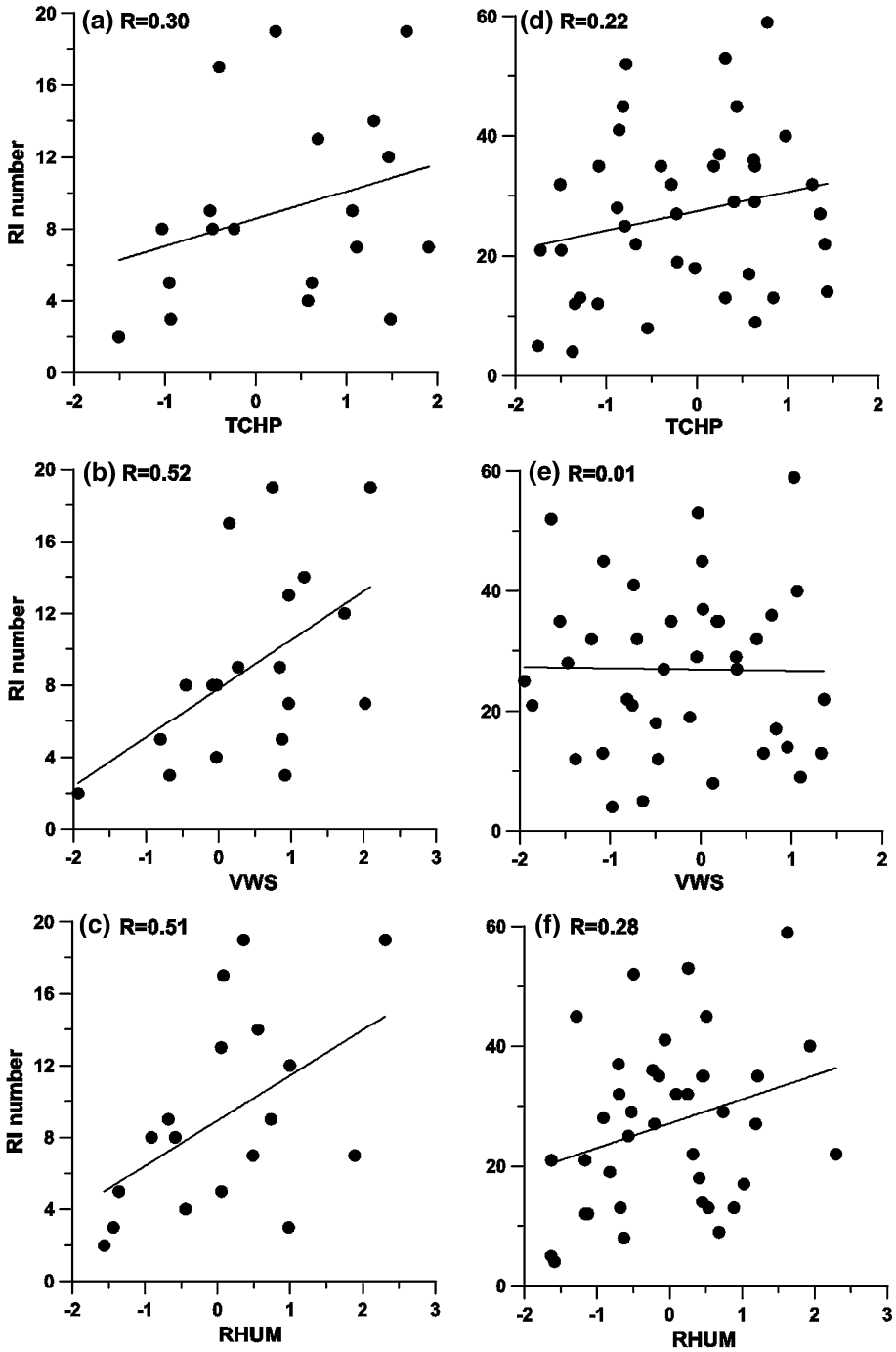

Fig. 4 Scatter diagrams between annual RI number and standardized PC1 of the averaged-May–November TCHP, VWS, and RHUM during warm (*right panel*) and cold (*left panel*) PDO phase. The *thick line* is the linear regression

at the 99 % confidence level by a Student's *t* test. Their EOF1s account for 33.4, 25.2, and 15.2 % of the total variance, respectively. EOF1 of TCHP is characterized by the east–west dipole structure, with high TCHP in the equatorial central and east Pacific and low TCHP in the equatorial west Pacific. This pattern is consistent with that found by Wada and Chan (2008). EOF1 of VWS reveals a pattern with the positive-negative-positive alternate distribution. This pattern is in agreement with that in Li and Zhou (2012), who had found a similar low VWS in the equatorial central and east Pacific. EOF1 of 500 hPa RHUM represents a southeast–northwest dipole-like structure.

To investigate the effects of the oceanic and atmospheric conditions associated with ENSO on the RI for the different PDO phases, we show the relationship between RI and standardized PC1 of TCHP, VWS, RHUM during the warm and cold PDO phase respectively (Fig. 4). The PC1 of TCHP reveals the positive correlation with RI in the both warm and cold phase, which is not statistically significant at the above 90 % confidence. It indicates that TCHP

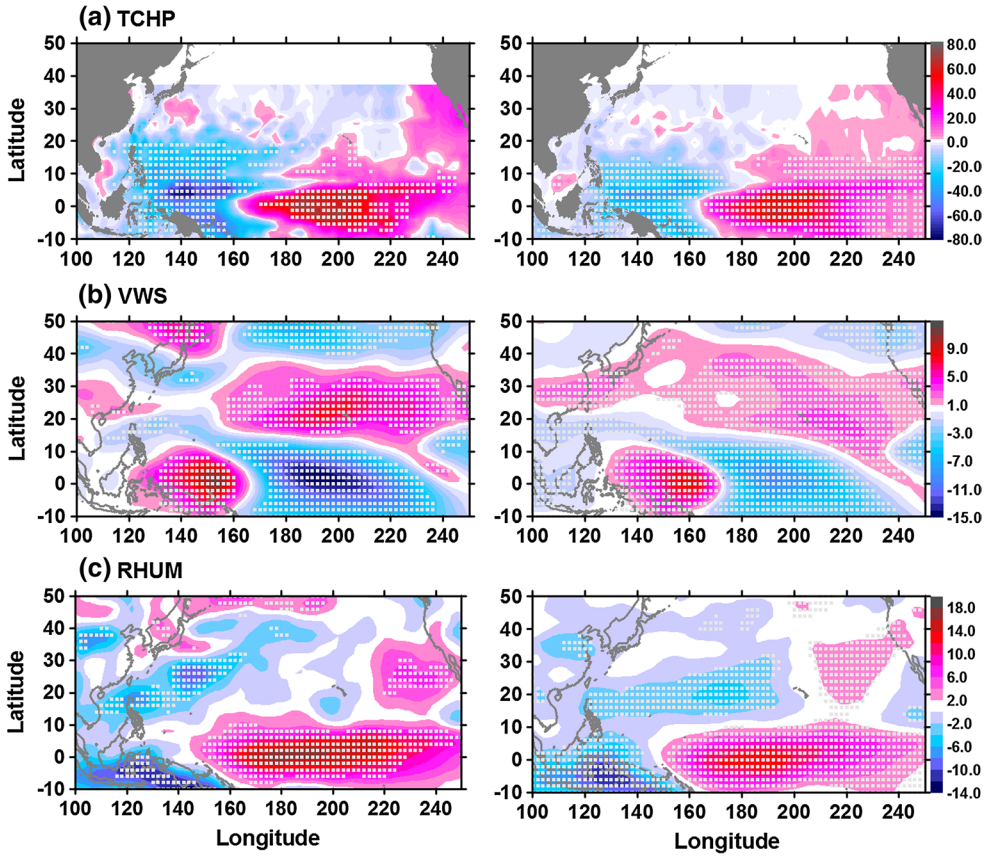

Fig. 5 Composite differences of averaged-May–November **a** TCHP, **b** VWS and **c** RHUM between El Niño and La Niña in the warm (*left panel*) and cold (*right panel*) phase of the PDO for the period 1951–2008. *Dots* indicate 95 % confidence level. See Table 1 for the El Niño and La Niña years for the composite difference

contributes less to the interannual ENSO–RI relationship change with the different PDO phases. The PC1 of VWS in the warm PDO phase is highly correlated with annual RI number, with significance at the 95 % confidence level, whereas the PC1 of VWS in the cold phase is hardly correlated with annual RI number. Similarly, the correlation (0.51) between the PC1 of RHUM and annual RI number in the warm PDO phase is much higher than that (0.28) in the cold PDO. The correlation in the warm PDO phase is statistically significant at the 95 % confidence level, but it is not in the cold PDO phase. These comparisons suggest that the atmospheric dynamic (VWS) and thermodynamic (RHUM) conditions play an important role in modulating the change of the interannual ENSO–RI relationship in the different PDO phases. It is noteworthy that atmospheric dynamic factor (VWS) may be dominant.

Figure 5 further shows the composite differences of TCHP, VWS and RHUM between the El Niño and La Niña years in the warm and cold PDO phase. The composite difference patterns of the three parameters between the El Niño and La Niña years for the different PDO phases are coherent with their respective EOF1s in Fig. 3. Moreover, the composite differences of the three parameters between the El Niño and La Niña years in the warm PDO phase show nearly same pattern as those in the cold PDO phase. However, most of the corresponding composite differences in the cold PDO phase are weakened, which indicates that the interannual variability of the TCHP, VWS and RHUM forced by ENSO in the North Pacific reduces in the cold PDO phase. We note that the cases selected for composite analysis are somewhat small for the La Niña years in the warm PDO phase. Therefore, we extend the period of 1951–2008 to 1900–2008 to confirm the results in Fig. 5, which is shown in Fig. 6. Three warm PDO phases (1900–1915, 1924–1943, and 1979–1997) and three cold PDO phases (1916–1923, 1951–1978 and 1998–2008) during 1900–2008 are obtained respectively. The pattern of composite difference during 1900–2008 is coherent with those in Fig. 5, indicating the same conclusion.

To determine how atmospheric circulations in association with RI change in the different PDO phases, composite differences of averaged-May–November 200 and 850 hPa wind vorticity between El Niño and La Niña in the warm and cold PDO phase are given in Fig. 7. It is shown that

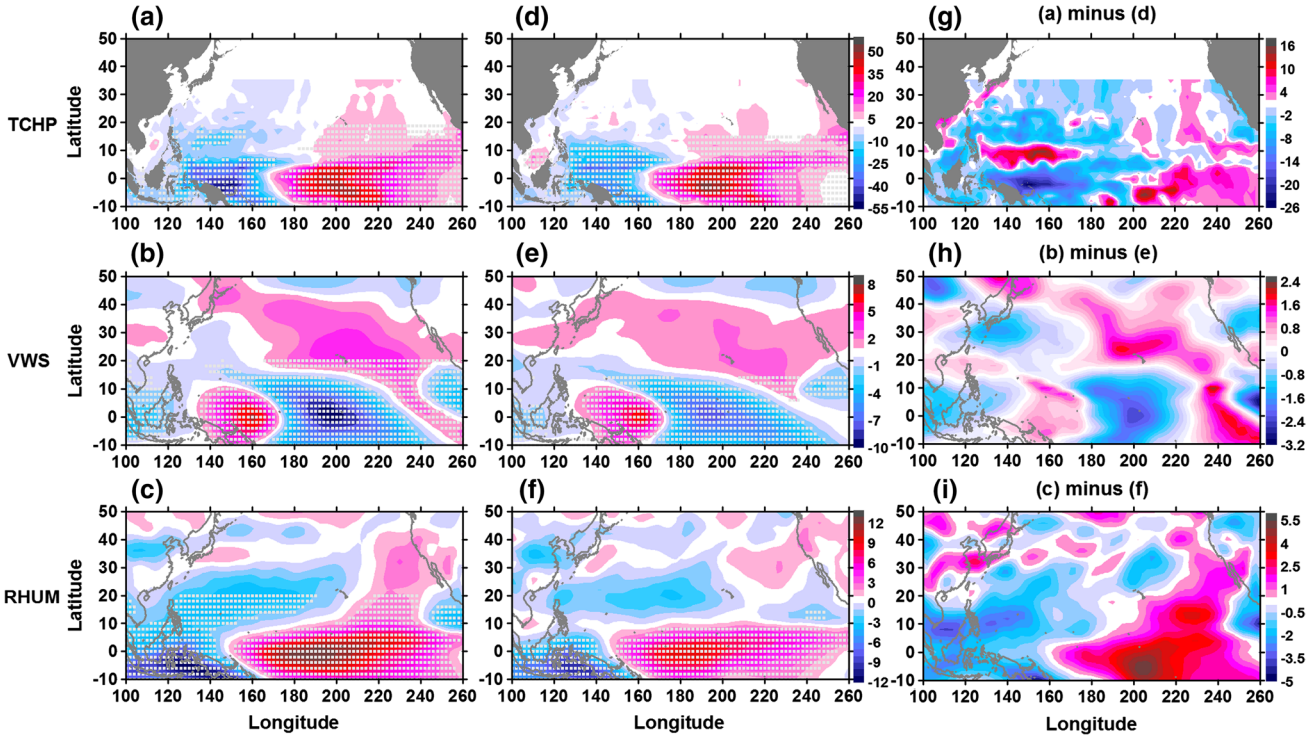

Fig. 6 Composite differences of averaged-May–November TCHP, VWS and RHUM between El Niño and La Niña in the warm (**a**–**c**) and cold (**d**–**f**) phase of the PDO for the period 1900–2008. **g**–**i** Differences between (**a**) and (**d**), (**b**) and (**e**), (**c**) and (**f**), respectively. *Dots* indicate 95 % confidence level

over the tropical North Pacific from equator to about 20°N, there are upper-level anomalous anticyclone and low-level cyclone in the composite difference for both the warm and cold PDO phase. Such anomalous large-scale circulations tend to support more RI occurrence in El Niño years than in La Niña years (Wang and Zhou 2008). However, the corresponding difference between El Niño and La Niña is much stronger in the warm PDO phase than in the cold PDO, especially in the location with maximum anomalous cores. This may be therefore contributing to the enhanced ENSO–RI relationship in the interannual timescale for the warm PDO phase.

Previous studies have found that the tropical atmosphere circulation anomaly is forced by summer SST anomalies generated by midlatitude intrinsic atmospheric variability in the Pacific during the previous winter, which is called seasonal footprinting mechanism (Vimont et al. 2001, 2003a, b). The seasonal footprinting mechanism accounts for up to 70 % of the decadal variability along the equator (Vimont et al. 2003a). Seasonal footprinting can be invoked as a mechanism for the PDO to affect the tropics through the low pressure related to PDO in the North Pacific Ocean (Krishnamurthy and Krishnamurthy 2013). The composite ENSO SST anomaly structures for the different PDO phases calculated from ERSST are shown in Fig. 8. There are evidently spatial asymmetries between El Niño and La Niña events in both warm and cold PDO phases. During the warm PDO phase, positive SST anomaly of El Niño events are characterized by a wedge structure in the tropical central and eastern Pacific, attaching to the west coast of the United States whereas La Niña events is featured by a tongue of negative SST anomaly confined in the equatorial central and eastern Pacific. During the cold PDO phase, the spatial asymmetries between El Niño and La Niña still exist but are a reversal to that in the warm PDO phase. Namely, positive anomalies of El Niño events are more located in the equatorial central and eastern Pacific, representing a tongue pattern while negative anomalies of La Niña events are extending from equatorial central and eastern Pacific to the west coast of the United States. Compared with El Niño in the cold PDO phase, that in the warm PDO phase has much larger SST anomaly in the equatorial eastern Pacific from 220°E to 280°E. Thus, the warm (cold) PDO phase, with warm (cold) ocean anomaly in the equatorial central and eastern Pacific (Zhang et al. 1997), can enhance (weaken) an El Niño episode, increasing (reducing) the effects of the warm pool of water in the equatorial Pacific in TC season through local diabatic heating (Gill 1980). Figure 9a shows this process by exhibiting

the different Walker circulation patterns associated with El Niño in the different PDO phases. It is shown that the El Niño events have stronger low-level convergence and upper-level divergence near dateline in the warm PDO phase than in the cold PDO phase, which is indicative of the enhanced ascending branch of Walker circulation in the warm PDO phase (Fig. 9a). However, PDO phase have no obvious effect on the Walker circulation pattern corresponding to La Niña events (Fig. 9b) as its ascending branch is located at far western tropical Pacific. It is found in turn that the convection over the central equatorial Pacific increases in the warm PDO phase (Fig. 9c) while it reduces in the cold PDO phase (Fig. 9d). Actually, this phenomena have also been discovered through the regression of PDO index onto the zonal mass streamfunction computed from zonal winds averaged over 5°S–5°N (Krishnamurthy and Krishnamurthy 2013). This tends to make the atmospheric response to ENSO stronger in the warm PDO phase (Fig. 9c) and weaker in the cold PDO phase (Fig. 9d), and so is the atmospheric teleconnection of ENSO (Figs. 7, 9c, d). Therefore it explains the weakened interannual ENSO–RI relationship in the cold PDO phase and strengthened interannual ENSO–RI relationship in the warm PDO phase.

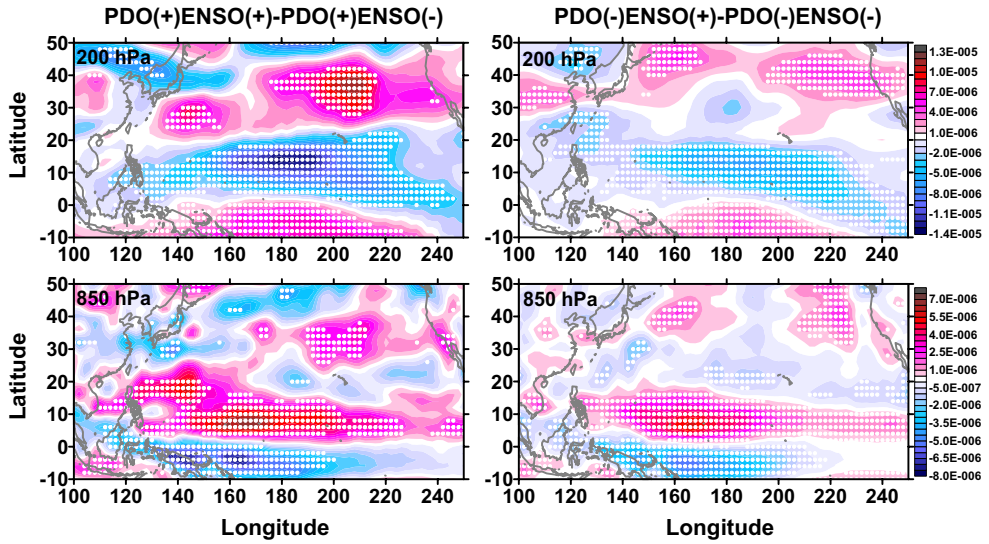

Fig. 7 Composite differences of averaged-May–November 200 hPa (*upper panel*) and 850 hPa (*lower panel*) vorticity between El Niño and La Niña in the warm (*left panel*) and cold (*right panel*) phase of the PDO for the period of 1951–2008. *Dots* indicate 95 % confidence level. See Table 1 for the El Niño and La Niña years for the composite difference

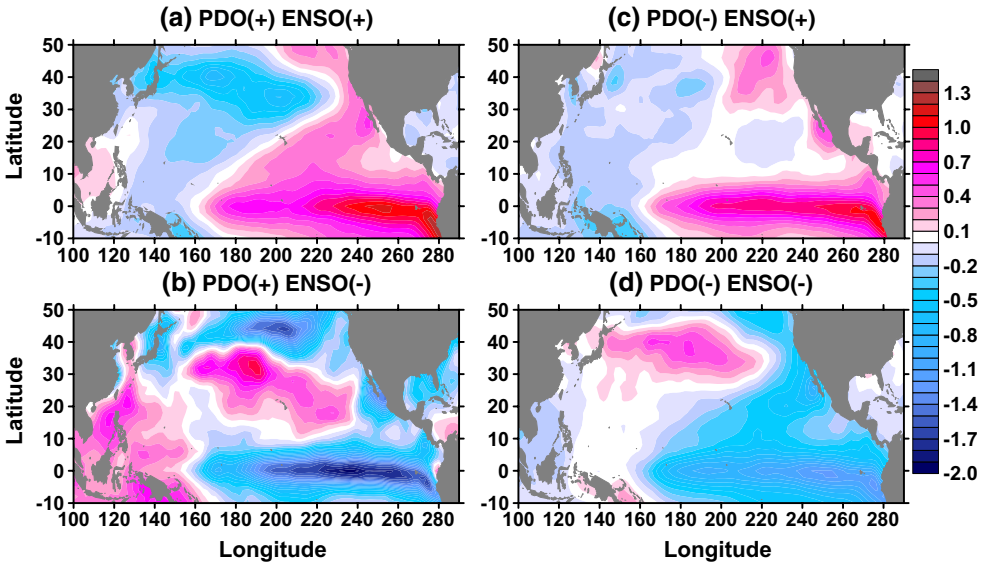

Fig. 8 Composite SST anomalies of **a** El Niño and **b** La Niña in the warm PDO phase, and **c** El Niño and **d** La Niña in the cold PDO phase. See Table 1 for the El Niño and La Niña years for the composite anomaly. The SST anomaly is calculated by subtracting climatological mean for May–November during 1951–2008 from SST of El Niño or La Niña

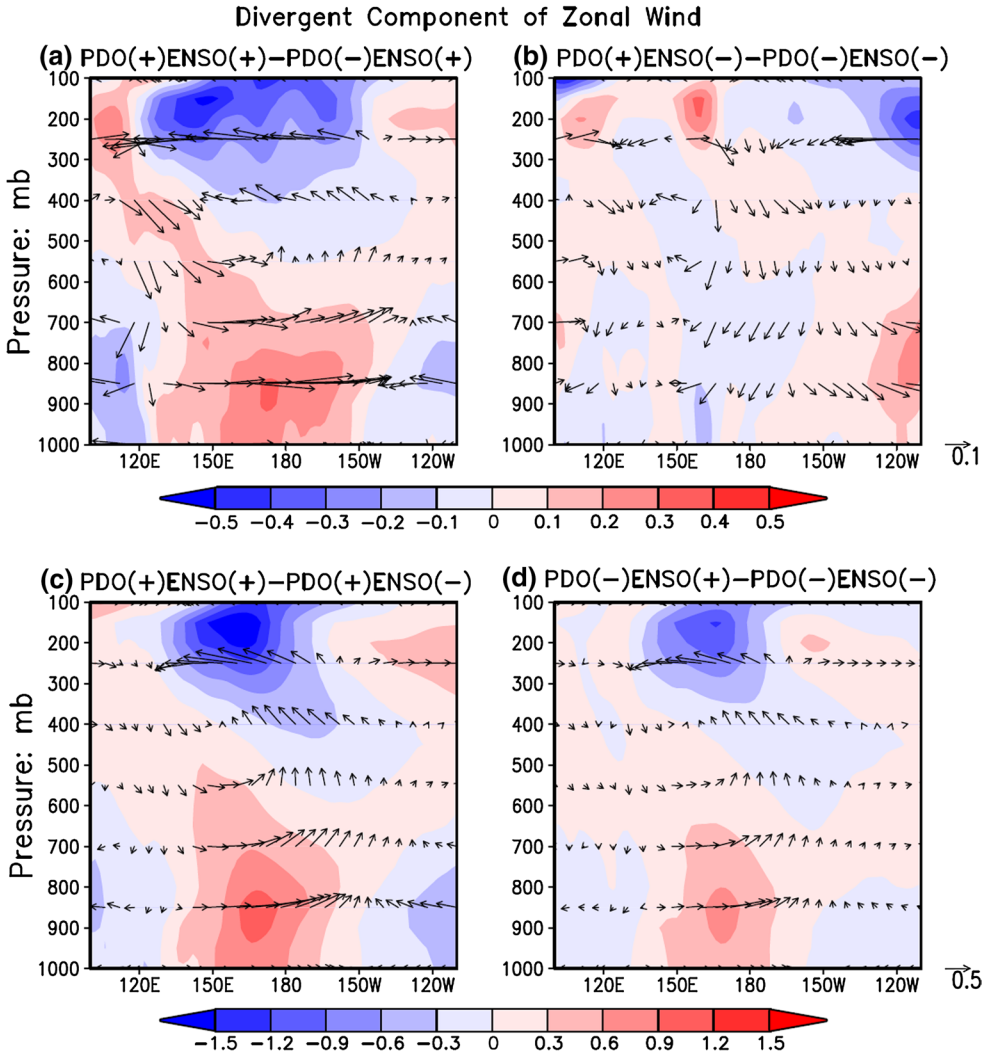

Fig. 9 Composite differences of averaged-May–November divergent component of zonal winds (*shading*) and Walker circulation (*vector*) during the period of 1951–2008 **a** between warm and cold phase of the PDO for the El Niño events, **b** between warm and cold phase of the PDO for the La Niña events, **c** between El Niño and La Niña in the warm PDO phase, **d** between El Niño and La Niña in the cold PDO phase. The unit of zonal winds is m/s. The *vertical velocity* is taken to be the negative of the pressure vertical velocity and its unit is 10 Pa/s

5 Summary and discussion

The PDO modulation of the interannual ENSO–RI relationship has been addressed for the first time in the present study. We identify that the interannual relationship between ENSO and annual RI number is strong and statistically significant when the PDO is in its warm phase. In contrast, when the PDO is in its cold phase, there is no significant relationship between ENSO and annual RI number on the interannual timescale. Therefore, the phase of PDO should be considered when we use ENSO as a predictor for the RI forecast, which may significantly improve the RI forecast accuracy.

The strength and frequency of ENSO events vary in relation with the PDO, which modulates the thermal and dynamic state of ocean and atmosphere on the multidecadal scale. Comparing with that in cold PDO phase, the interannual variability of TCHP, VWS and RHUM related to RI is strengthened in warm PDO phase. However, correlations between the PC1 of TCHP and annual RI number in the either PDO phase are not statistically significant at the above 90 % confidence. Therefore, it is suggested that TCHP less affect the interannual ENSO–RI relationship change with different PDO phases. In contrast, VWS and RHUM in the warm PDO phase are more highly correlated with the annual RI number than in the cold PDO phase. Besides, their correlation is statistically significant at the 95 % confidence level in the warm PDO phase, but it is not in the cold phase. Therefore, these results confirm that

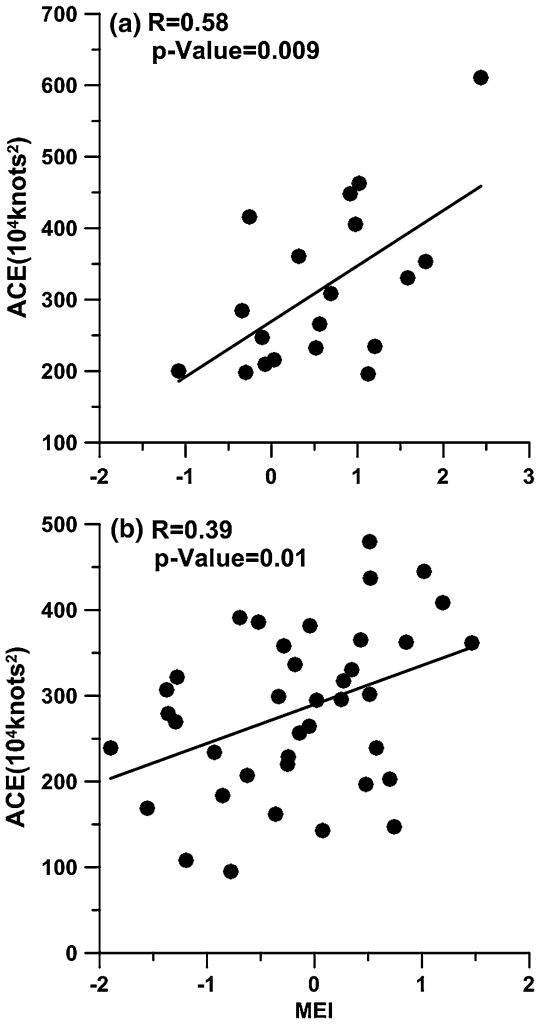

Fig. 10 Scatter diagrams between the averaged-May–November MEI and annual ACE for the **a** warm and **b** cold PDO phase. The *thick line* is the linear regression

VWS and RHUM play direct roles in causing the strong interannual ENSO–RI relationship in the warm PDO phase. Based on the correlation analysis, it is also found that VWS may be a determinant factor in modulating interannual ENSO–RI relationship, which indicates the dominance of atmospheric dynamic conditions.

The mechanisms by which the PDO modulates the effects of ENSO on large-scale atmospheric environment related to RI are investigated. Analysis demonstrates that the warm (cold) PDO phase can strengthen (weaken) an El Niño event, increasing (reducing) the effects of the warm pool of water over the equatorial Pacific in TC season through local diabatic heating. El Niño events are accompanied by the stronger Walker circulation in the equatorial Pacific in the warm PDO phase than in the cold PDO phase. In contrast, the Walker circulation pattern in association with La Nina events is less affected by the alternate PDO phase. This tends to make the atmospheric response to ENSO stronger (weaker) in warm (cold) PDO phase, and so is the atmospheric teleconnection of ENSO. Hence, it contributes to the enhanced (weakened) interannual ENSO–RI relationship in the warm (cold) PDO phase.

In this study, 80 % of the STs (category 4–5 TCs) experience at least one RI process which accounts for 51 % of TCs with RI event. The time evolution of annual RI and ST number is considerably similar, with the correlation coefficient of 0.54, which is statistically significant at the 99 % confidence level (not shown). Thus, it is likely that the present findings may also be an important implication to the statistical forecast of ST. Certainly, it is necessary to investigate further. Due to 80 % of the STs with at least one RI event, a better understanding of climate variability of RI events may shed light on the mechanism responsible for the climate variability in the STs.

Many studies showed that ENSO has obvious interdecadal and decadal variations in its frequency and intensity (e.g., An and Wang 2000; Yeh and Kirtman 2004). In addition to extratropical Pacific Ocean forcing such as PDO by footprinting mechanism, decadal ENSO variability could originate internally within the tropics (e.g., Penland and Sardeshmukh 1995; Knutson et al. 1997; Newman 2007; Sun and Yu 2009; Yu and Kim 2011). Interactions between ENSO and the tropical Pacific mean state is considered as one of the tropics-origin mechanisms for decadal ENSO variability (Sun and Yu 2009; Yu and Kim 2011). Recent studies have also argued that ENSO itself has experienced decadal changes during the past decades. For example, it is suggested that the frequency of the central Pacific El Niño events increased noticeably since 1990 (Yeh et al. 2009; Lee and McPhaden 2010). Several studies have confirmed that atmospheric teleconnections associated with the central Pacific El Niño and eastern Pacific El Niño events represent different characteristics (Kim et al. 2009; Weng et al. 2009). These imply that the PDO may not be the sole source that modulates the interannual influence of ENSO on the RI. The decadal variability of the ENSO and associated atmospheric teleconnections are complex with multiple aspects. How it modulates the oceanic and atmospheric states to impact on TC RI need to be further investigated.

In this study, we mainly focus on the PDO modulation of the interannual ENSO–RI relationship. Earlier studies found that ACE in the WNP is positively correlated with ENSO (e.g., Camargo and Sobel 2005). In fact, it is interesting to note how PDO modulates the interannual ENSO–ACE relationship in the WNP. ACE represents the integrated characteristics of the number, lifetimes, and intensities of TCs occurring in a basin over a given period of time (Camargo and Sobel 2005). Here, the ACE of a TC season is calculated by summing the squares of the estimated maximum sustained wind speed of every active

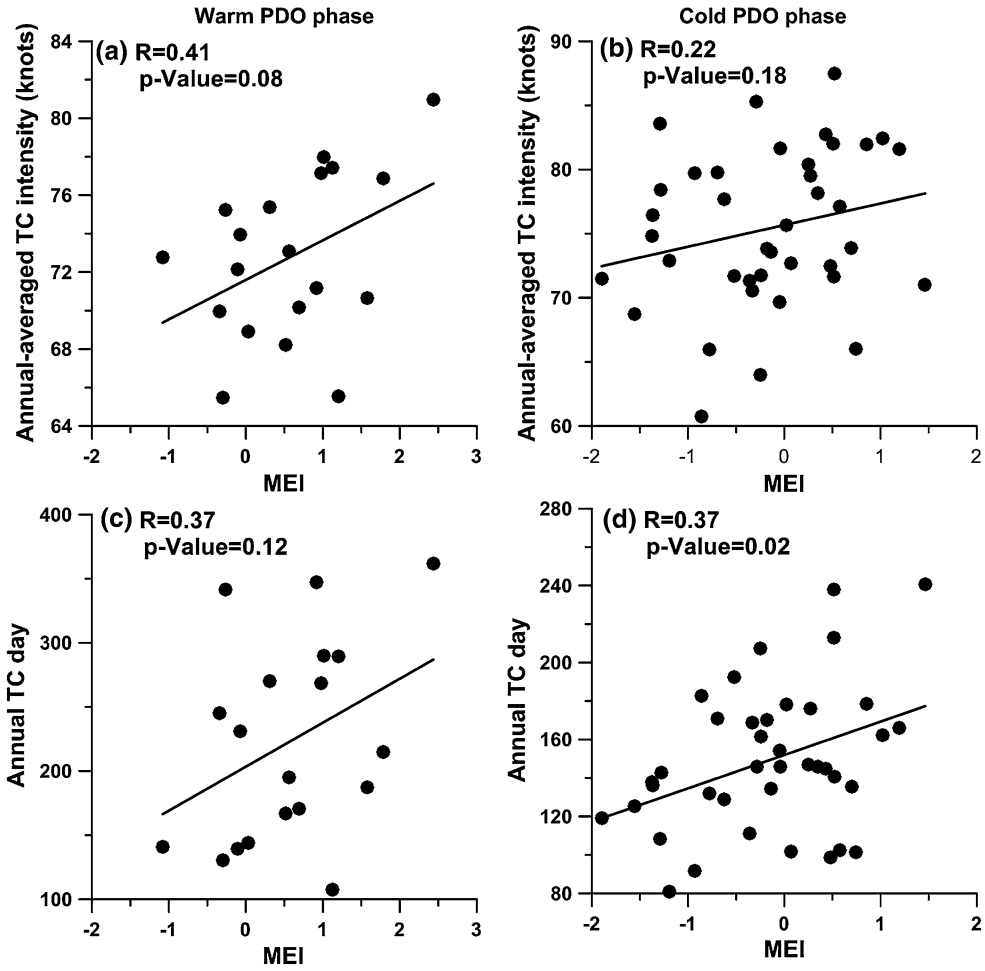

Fig. 11 Scatter diagrams between averaged-May–November MEI and annual-averaged TC intensity, and annual TC day for the **a**, **c** warm and **b**, **d** cold PDO phases. Based on *t* distribution, the *p* value is calculated. The *thick line* is the linear regression

tropical storm (wind speed 35 knots or higher), at 6-h intervals. If any storms of a TC season happen to cross years, the TC's ACE counts for the previous year. Figure 10 shows the relationship between the averaged-May–November MEI and annual ACE in the different PDO phases. The correlation coefficients between the MEI and ACE during the warm and cold PDO phase are 0.58, and 0.39, respectively (Fig. 10). Based on *t* distribution, we calculate the *p* value of the correlations in the different PDO phases. The *p* value is 0.009 (0.01) in the warm (cold) phase. Thus, difference of the effect of the different PDO phases on the interannual relationship between ENSO and ACE may be negligibly small. What causes the lack of PDO effect on ENSO–ACE relationship? Since the ACE is a combination of TC intensity, number and duration, we examine the relationships between averaged-May–November MEI and annual-averaged TC intensity, and annual TC day in the different PDO phases. It is shown that the correlation (R = 0.41, *p* value = 0.08) between MEI and annual-averaged TC intensity in the warm PDO phase is more significant than that (R = 0.22, *p* value = 0.18) in the cold PDO phase. In contrast, the correlation (R = 0.37, *p* value = 0.02) between MEI and annual TC day in the cold PDO phase is more significant than that (R = 0.37, *p* value = 0.12) in the warm PDO phase (Fig. 11). Thus, this confirms that the lack of PDO effect on ENSO–ACE relationship may be because the effect of PDO on the relationship between the TC lifetime and ENSO counteracts that between the TC intensity and ENSO. The specific mechanism needs to investigate further in the future study.

Acknowledgments This study was jointly supported by the National Basic Research Program of China (2013CB430304), National Natural Science Foundation (41376015, 41376013, 41306006, 41206178, and 41176003) of China, and National High-Tech R&D Program (2013AA09A505) of China, and Global Change and Air-Sea Interaction (GASI-01-01-12) of China. H. Liu's work was supported by the University of Miami's Cooperative Institute for Marine and Atmospheric Studies (Cooperative Agreement #NA10OAR4320143) and NOAA's Atlantic Oceanographic and Meteorological Laboratory. The 6-h tropical cyclone best-track data is obtained from the Joint Typhoon Warning Center (http://www.usno.navy.mil/JTWC/). SODA data is downloaded from web site at http://

dsrs.atmos.umd.edu/DATA/soda_2.2.4/. The twentieth century Reanalysis V2 data is provided by the NOAA/OAR/ESRL PSD, Boulder, Colorado, USA, from their Web site at http://www.esrl.noaa.gov/psd/.

References

An SI, Wang B (2000) Interdecadal change of the structure of the ENSO mode and its impact on the ENSO frequency. J Clim 13:2044–2055

Ashok K, Yamagata T (2009) Climate change: the El Niño with a difference. Nature 461:481–484

Ashok K, Behera SK, Rao SA, Weng H, Yamagata T (2007) El Niño Modoki and its possible teleconnection. J Geophys Res 112:C11007. doi:10.1029/2006JC003798

Camargo SJ, Sobel AH (2005) Western North Pacific tropical cyclone intensity and ENSO. J Clim 18:2996–3006

Camargo SJ, Robertson AW, Gaffney SJ, Smyth P, Ghil M (2007) Cluster analysis of typhoon tracks: part II: largescale circulation and ENSO. J Clim 20:3654–3676

Compo GP et al (2011) The twentieth century reanalysis project. Q J R Meteorol Soc 137:1–28

Elsner JB, Liu KB (2003) Examining the ENSO typhoon hypothesis. Clim Res 25:43–54

Gill AE (1980) Some simple solutions for heat-induced tropical circulation. Q J R Meteorol Soc 106:447–462

Kao HY, Yu JY (2009) Contrasting Eastern Pacific and Central Pacific types of ENSO. J Clim 22:615–631

Kaplan J, DeMaria M (2003) Large-scale characteristics of rapidly intensifying tropical cyclones in the north Atlantic basin. Weather Forecast 18:1093–1108

Kaplan J, DeMaria M, Knaff JA (2010) A revised tropical cyclone rapid intensification index for the Atlantic and East Pacific basins. Weather Forecast 25:220–241

Kim HM, Webster PJ, Curry JA (2009) Impact of shifting patterns of Pacific ocean warming on North Atlantic tropical cyclone. Science 325:77–80

Kim HM, Webster PJ, Curry JA (2011) Modulation of north Pacific tropical cyclone activity by three phases of ENSO. J Clim 24:1839–1849

Knutson TR, Manabe S, Gu D (1997) Simulated ENSO in a global coupled ocean–atmosphere model: multidecadal amplitudemodulation and CO_2 sensitivity. J Clim 10:131–161

Krishnamurthy L, Krishnamurthy V (2013) Influence of PDO on South Asian summer monsoon and monsoon–ENSO relation. Clim Dyn. doi:10.1007/s00382-013-1856-z

Kug JS, Jin FF, An SI (2009) Two types of El Nino events: cold Tongue El Niño and warm pool El Niño. J Clim 22:1499–1515

Kurtzman D, Scanlon BR (2007) El Niño-Southern Oscillation and Pacific Decadal Oscillation impacts on precipitation in the southern and central United States: evaluation of spatial distribution and predictions. Water Resour Res 43:W10427. doi:10.1029/2007WR005863

Lee T, McPhaden MJ (2010) Increasing intensity of El niño in the central-equatorial Pacific. Geophys Res Lett 37:L14603. doi:10.1029/2005GL022860

Li RCY, Zhou W (2012) Changes in western Pacific tropical cyclones associated with the El niño–Southern oscillation cycle. J Clim 25:5864–5878. doi:10.1175/JCLI-D-11-00430.1

Lin I-I, Wu CC, Pun IF, Ko DS (2008) Upper-ocean thermal structure and the western North Pacific category 5 typhoons. Part I: ocean features and the category 5 typhoons' intensification. Mon Weather Rev 136(9):3288–3306

Mantua NJ, Hare SR, Zhang Y, Wallace JM, Francis RC (1997) A Pacific interdecadal climate oscillation with impacts on salmon production. Bull Am Meteorol Soc 78(6):1069–1079

Newman M (2007) Interannual to decadal predictability of tropical and North Pacific sea surface temperatures. J Clim 20:2333–2356

Penland C, Sardeshmukh PD (1995) The optimal growth of tropical sea surface temperature anomalies. J Clim 8:1999–2024

Shu SJ, Ming J, Chi P (2012) Large-scale characteristics and probability of rapidly intensifying tropical cyclones in the western north pacific basin. Weather Forecast 27:411–423

Smith TM, Reynolds RW, Peterson TC, Lawrimore J (2008) Improvements to NOAA's historical merged land-ocean surface temperature analysis (1880–2006). J Clim 21:2283–2296

Sun F, Yu JY (2009) A 10–15-yr modulation cycle of ENSO intensity. J Clim 22:1718–1735

Verdon DC, Franks SW (2006) Long-term behaviour of ENSO: interactions with the PDO over the past 400 years inferred from paleoclimate records. Geophys Res Lett 33:L06712. doi:10.1029/2005GL025052

Vimont DJ, Battisti DS, Hirst AC (2001) Footprinting: a seasonal connection between the tropics and midlatitudes. Geophys Res Lett 28:3923–3926

Vimont DJ, Battisti DS, Hirst AC (2003a) The seasonal footprinting mechanism in the CSIRO general circulation models. J Clim 16:2653–2667

Vimont DJ, Wallace JM, Battisti DS (2003b) The seasonal footprinting mechanism in the Pacific: implications for ENSO. J Clim 16:2668–2675

Wada A, Chan JCL (2008) Relationship between typhoon activity and upper ocean heat content. Geophys Res Lett 35:L17603. doi:10.1029/2008GL035129

Wang B, Chan JCL (2002) How strong ENSO events affect tropical storm activity over the western North Pacific. J Clim 15:1643–1658

Wang CZ, Wang X (2013) Classifying El Niño Modoki I and II by different impacts on rainfall in Southern China and typhoon tracks. J Clim 26(4):1322–1338

Wang B, Zhou X (2008) Climate variation and prediction of rapid intensification in tropical cyclones in the western North Pacific. Meteorol Atmos Phys 99:1–16. doi:10.1007/s00703-006-0238-z

Wang L, Chen W, Huang R (2008) Interdecadal modulation of PDO on the impact of ENSO on the east Asian winter monsoon. Geophys Res Lett 35:L20702. doi:10.1029/2008GL035287

Wang X, Wang D, Zhou W (2009) Decadal variability of twentieth-century El Niño and La Niña occurrence from observations and IPCC AR4 coupled models. Geophys Res Lett 36:L11701. doi:10.1029/2009GL037929

Wang CZ, Li CX, Mu M, Duan WS (2013) Seasonal modulations of different impacts of two types of ENSO events on tropical cyclone activity in the western North Pacific. Clim Dyn 40(11–12):2887–2902

Wang X, Zhou W, Li C, Wang D (2014) Comparison of the impact of two types of El Niño on tropical cyclone genesis over the South China Sea. Int J Climatol 34:2651–2660

Weng H, Ashok K, Behera SK, Rao AS, Yamagata T (2007) Impacts of recent El Niño Modoki on dry/wet conditions in the Pacific rim during boreal summer. Clim Dyn 29:113–129

Weng H, Ashok K, Behera SK, Yamagata T (2009) Anomalous winter climate conditions in the Pacific rim during recent El Niño Modoki and El Niño events. Clim Dyn 29:113–129

Wolter K, Timlin MS (1998) Measuring the strength of ENSO events: how does 1997/98 rank? Weather 53:315–324

Wu R, Wang B (2002) A contrast of the east Asian summer monsoon–ENSO relationship between 1962–77 and 1978–93. J Clim 15(22):3266–3279

Yeh SW, Kirtman BP (2004) Tropical Pacific decadal variability and ENSO amplitude modulation in a CGCM. J Geophys Res 109:C11009. doi:10.1029/2004JC002442

Yeh SW, Kug JS, Dewitte B, Kwon MH, Kirtman BP, Jin FF (2009) El Niño in a changing climate. Nature 461:511–514

Yu JY, Kim ST (2011) Reversed spatial asymmetries between El Niño and La Niña and their linkage to decadal ENSO modulation in CMIP3 models. J Clim 24:5423–5434

Yu B, Zwiers FW (2007) The impact of combined ENSO and PDO on the PNA climate: a 1,000-year climate modeling study. Clim Dyn 29:837–851

Zhang Y, Wallace JM, Battisti DS (1997) ENSO-like interdecadal variability: 1900–93. J Clim 10:1004–1020